Diabetologia (2024) 67:1683–1697
https://doi.org/10.1007/s00125-024-06180-x

ARTICLE

Capillary contact points determine beta cell polarity, control secretion and are disrupted in the *db*/*db* mouse model of diabetes

Dillon Jevon[1] · Louise Cottle[1] · Nicole Hallahan[1] · Richard Harwood[2] · Jaswinder S. Samra[3,4] · Anthony J. Gill[3,5,6] · Thomas Loudovaris[7] · Helen E. Thomas[7,8] · Peter Thorn[1]

Received: 11 January 2024 / Accepted: 26 March 2024 / Published online: 30 May 2024

Abstract

Aims/hypothesis Almost all beta cells contact one capillary and insulin granule fusion is targeted to this region. However, there are reports of beta cells contacting more than one capillary. We therefore set out to determine the proportion of beta cells with multiple contacts and the impact of this on cell structure and function.

Methods We used pancreatic slices in mice and humans to better maintain cell and islet structure than in isolated islets. Cell structure was assayed using immunofluorescence and 3D confocal microscopy. Live-cell two-photon microscopy was used to map granule fusion events in response to glucose stimulation.

Results We found that 36% and 22% of beta cells in islets from mice and humans, respectively, have separate contact with two capillaries. These contacts establish a distinct form of cell polarity with multiple basal regions. Both capillary contact points are enriched in presynaptic scaffold proteins, and both are a target for insulin granule fusion. Cells with two capillary contact points have a greater capillary contact area and secrete more, with analysis showing that, independent of the number of contact points, increased contact area is correlated with increased granule fusion. Using *db*/*db* mice as a model for type 2 diabetes, we observed changes in islet capillary organisation that significantly reduced total islet capillary surface area, and reduced area of capillary contact in single beta cells.

Conclusions/interpretation Beta cells that contact two capillaries are a significant subpopulation of beta cells within the islet. They have a distinct form of cell polarity and both contact points are specialised for secretion. The larger capillary contact area of cells with two contact points is correlated with increased secretion. In the *db*/*db* mouse, changes in capillary structure impact beta cell capillary contact, implying that this is a new factor contributing to disease progression.

Keywords Beta cell · Diabetes · Human · Insulin · Islet · Polarity

Abbreviations

Dlg	Discs large
E-cadherin	Epithelial cadherin
ECM	Extracellular matrix
KRBH	Krebs Ringer bicarbonate buffer
Par3	Partitioning defective protein 3
pFAK	Phosphorylated focal adhesion kinase
ROI	Region of interest
SRB	Sulforhodamine B

✉ Peter Thorn
p.thorn@sydney.edu.au

[1] Charles Perkins Centre, School of Medical Sciences, University of Sydney, Camperdown, NSW, Australia

[2] Charles Perkins Centre, Sydney Microscopy and Microanalysis, University of Sydney, Camperdown, NSW, Australia

[3] The University of Sydney Northern Clinical School, Sydney, NSW, Australia

[4] Upper Gastrointestinal Surgical Unit, Royal North Shore Hospital, St Leonards, NSW, Australia

[5] Department of Anatomical Pathology, Royal North Shore Hospital, St Leonards, NSW, Australia

[6] Cancer Diagnosis and Pathology Research Group, Kolling Institute of Medical Research, St Leonards, NSW, Australia

[7] St Vincent's Institute, Fitzroy, VIC, Australia

[8] Department of Medicine, St Vincent's Hospital, University of Melbourne, Fitzroy, VIC, Australia

Research in context

What is already known about this subject?

- Beta cells orientate with respect to capillaries with three distinct spatial domains: basal, lateral and apical. These are defined by polar determinants, such as scribble, Dlg and Par3, and by local enrichment of synaptic scaffold proteins, such as liprin and ELKS
- Beta cells can contact more than one capillary
- Changes in islet capillary structure are characteristic of type 2 diabetes but the impact on beta cells is unknown

What is the key question?

- How are beta cells influenced by contacts with islet capillaries?

What are the new findings?

- A significant proportion of beta cells in mouse and human islets have two points of capillary contact. These cells have a distinct form of polarity and each capillary contact is enriched in presynaptic scaffold proteins and is a target for insulin granule fusion
- The greater the beta cell capillary contact area, the higher the number of granule fusion events
- In islets from *db/db* mice, changes in capillary organisation are associated with reductions in total capillary area and contact area for each beta cell

How might this impact on clinical practice in the foreseeable future?

- This work adds further evidence on the importance of the environment for beta cell function, which will inform the development of cell-based cures for type 1 diabetes. It also highlights that changes to capillaries in type 2 diabetes can affect beta cell structure, which could lead to better treatment strategies

Introduction

Indirect data suggest beta cells might be polarised, with evidence of polar distribution of viral particles [1], insulin granules [2] and the Golgi apparatus [3]. More recently, a regulator of cell polarity, liver kinase B1 (LKB1), was shown to control beta cell structure [4], and direct evidence shows segregated distributions of polarity determinant complexes indicating a basal region at the capillary interface, a lateral region where endocrine cells contact each other and an apical region that defines luminal spaces into which each beta cell projects a primary cilium [5].

This polar organisation of beta cells is paralleled by the spatial organisation of functional domains. The GLUT2 transporter is enriched laterally [6], ribosomes [7] and primary cilia [5, 8] are apical and presynaptic scaffold proteins are enriched basally at the interface with the capillary [5, 9, 10]. These presynaptic scaffold proteins, such as ELKS, liprin and Rab interacting molecule 2 (RIM2), are important in controlling insulin secretion [11–14] and their enrichment at the capillary interface spatially coincides with targeting of insulin granule fusion to the capillaries [10]. The mechanisms that orientate and organise beta cell structure are unknown. The contact point of the beta cell with the capillaries is the only region where beta cells interact with the extracellular matrix (ECM) [9, 15, 16]. This locally activates integrins [9] and, by analogy with the mechanisms that polarise epithelial cells, could trigger sorting mechanisms to define this as the basal domain [17].

The environment of the islet is complex, with a tortuous and tightly packed capillary bed [18]. Bonner-Weir [2] and our laboratory [5] have reported that, as a result, beta cells can have multiple points of contact with the islet capillaries, with previous speculation that each contact point might have different functions [2]. An obvious question then is, what does cell polarity look like in these beta cells and what consequence might it have for beta cell structure and function?

Furthermore, in type 2 diabetes the islet capillary bed and endothelial cells undergo changes [19–23]. It would seem natural that these changes might have a consequence for the interaction of beta cells with the capillaries and potentially an impact on beta cell function.

Methods

Animal husbandry Mice were housed at the Charles Perkins Centre in a pathogen-free environment, at 22°C with 12 h light cycles and a chow diet. Mice (8–12 weeks old) were humanely killed according to animal ethics procedures

(University of Sydney Ethics Committee, no. 20191642 and no. 2023/2300).

Male LepR$^{db/db}$ mice were genotyped and phenotyped (B6.BKS(D)-*Lepr*^{db}/J [The Jackson Laboratory, USA; https://www.jax.org/strain/000697]). Diabetes severity was classified based on AUC analysis of IPGTTs, beginning at stage 1 with compensation (AUC <1600 mmol/l × min) and ending at stage 4 with severe diabetes (AUC >2800 mmol/l × min) (see [24] for details). All LepR$^{db/db}$ mice in this work exhibited stage 4 type 2 diabetes at 12 weeks.

Human pancreatic tissue Human pancreatic tissue was sourced from pancreatic tumour resections or cadaveric donors. Tumour resections were performed at the Royal North Shore Hospital and tissue was collected with patient consent, approved by the Northern Sydney Local Health District Human Research Ethics Committee. Fixed pancreatic sections were from the JDRF Network for Pancreatic Organ donors with Diabetes (nPOD) tissue bank, approved by the Human Research Ethics Committee at the University of Sydney. Cadaveric donor tissue and islets were sourced from St Vincent's Institute. Informed consent was acquired, and the study was approved by the Human Research Ethics Committee at the University of Sydney. Information on pancreatic tissue donors and islet donors/preparations is listed in electronic supplementary material (ESM) Table 1.

Pancreatic slicing The mouse pancreas was inflated by injecting 2 ml of 37°C 1% agarose (Ultrapure Low Melting Point, Invitrogen, ThermoFisher, Australia). The pancreas was excised, trimmed and placed into 15 mm × 15 mm × 5 mm tissue moulds (Tissue-Tek Cryomold, Sakura, Emgrid, Australia), and tissue blocks cast by pipetting 1 ml of 37°C 2% agarose and solidifying on ice.

Human pancreatic tissue was fixed using 4% paraformaldehyde (Sigma-Aldrich, Merck, Australia) at 4°C for 2.5 h. Tissue was washed before storage at 4°C in PBS supplemented with 0.01% sodium azide. Fixed tissue was mounted in 1.5% low-melting-point agarose as above.

Tissue blocks (mouse or human) were sectioned (150–200-µm-thick slices) on a vibratome (Leica VT1000s, Leica, Australia). For fixed-cell imaging experiments, mouse slices were then fixed in 0.5 ml of 4% paraformaldehyde and washed three times in PBS before being stained.

For live-cell assays, mouse slices were cultured in RPMI-1640 culture medium (Sigma-Aldrich), 10.7 mmol/l glucose, supplemented with 10% FBS (Gibco, ThermoFisher, Australia), 100 U/ml penicillin/0.1 mg/ml streptomycin (Invitrogen), 1 µM dexamethasone and 0.01% soybean trypsin inhibitor, overnight in an incubator (37°C, 95% air/5% CO_2), the medium being replaced 2 h after slicing.

Immunolabelling Fixed pancreatic slices were incubated in blocking buffer (3% BSA, 3% donkey serum, 0.3% Triton X-100) for 3 h at room temperature followed by primary antibody at 4°C overnight. Slices were washed three times in PBS and secondary antibodies in blocking buffer were added for 4 h at 4°C. After washing three times in PBS, tissues were mounted on slides with Prolong Diamond anti-fade (Invitrogen). Slides were stored at 4°C and imaged within 5 days.

Antibodies Primary antibodies are shown in Table 1. Secondary antibodies were goat anti-guinea pig Alexa Fluor 488, goat anti-mouse Alexa Fluor 546, goat anti-rabbit Alexa Fluor 594 and goat anti-rat Alexa Fluor 647 (Invitrogen), diluted 1:200 in blocking buffer. DAPI (Sigma-Aldrich, 100 ng/ml final concentration) was added with the secondary antibodies.

Confocal image acquisition Images were acquired on a Leica SP8 confocal microscope with a ×40 or ×63 oil immersion lens, and excited with tuneable white light and an ultraviolet laser. Z stacks were acquired at 255 nm intervals (mouse islets) or 336 nm intervals (human islets) over a depth of around 40 µm.

3D cell polarity analysis Cells with two capillary contacts were located in the confocal Z stacks. To quantify protein localisation at the basal, lateral and apical domains, 5-pixel-wide linescans were drawn along the cell membrane of each domain (Fiji [25]). Average fluorescence intensity of the line was measured on multiple Z planes, and the average intensity of measurements over all planes was calculated for each

Table 1 Primary antibodies

Target	Species	Dilution	Identifier
Insulin	Guinea pig	Stock	Agilent, A0564; RRID:AB_10013624
Dlg	Mouse	1:200	BD Biosciences, 610874; RRID:AB_398191
E-cadherin	Mouse	1:200	BD Biosciences, 610181; RRID:AB_397580
ELKS	Mouse	1:200	Abcam, Ab50312; RRID:AB_869944
Laminin beta-1	Rat	1:200	Thermo Fisher, MA5-14657; RRID:AB_10981503
Liprin α1	Rabbit	1:200	Proteintech, 14175-2-AP; RRID:AB_2171592
Par3	Rabbit	1:200	Millipore, 07-330; RRID:AB_2101325
pFAK (Y397)	Rabbit	1:100	Cell Signaling, 8556; RRID:AB_10891442

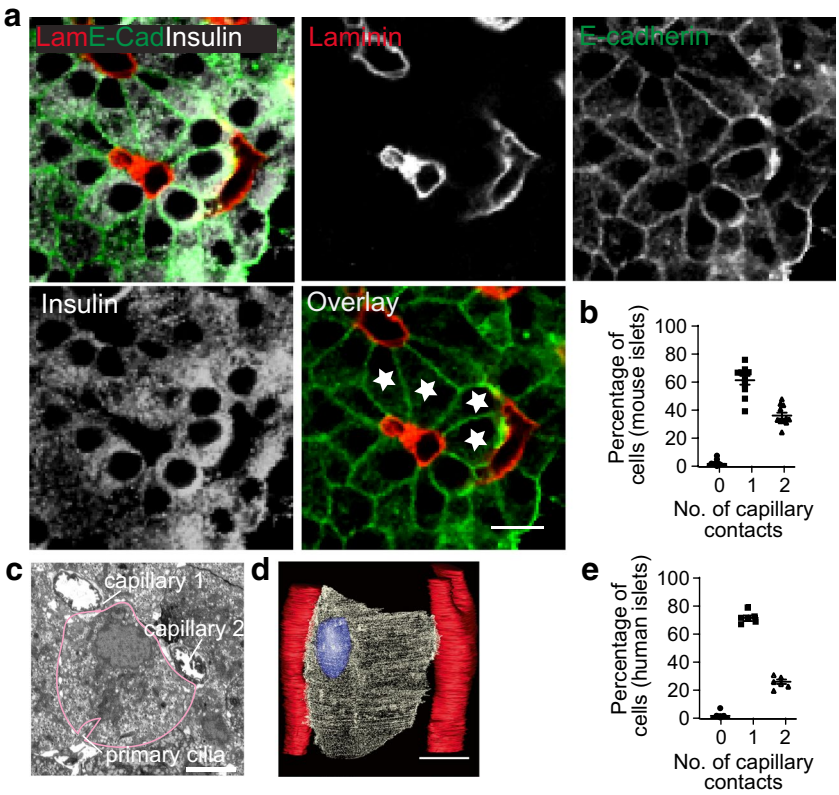

Fig. 1 Beta cells contacting two capillaries are a significant proportion of the total beta cell population. (**a**) Laminin (Lam) immunostaining identifies islet capillaries, insulin the beta cells and E-cadherin (E-cad) the cell outlines. Many beta cells contact two capillaries, for example, those identified with a star in the overlay image. (**b**) In mouse islets, within a pancreatic slice, serial confocal sections identify that 36% of cells contact two capillaries (n=11 islets, 858 beta cells, 6 mice). (**c**) An example electron micrograph of a single beta cell contacting two capillaries. Scale bar, 5 µm. (**d**) Reconstruction of serial electron micrograph sections showing a single beta cell and two capillary contacts. Scale bar, 5 µm. (**e**) In human islets, within slices, 22% of beta cells contact two capillaries (n=5 islets from 2 donors, 262 beta cells)

fluorescence channel of interest at every domain. For each channel, the sum of the fluorescence intensities in all these regions was calculated. The fluorescence intensity calculated for each domain was then expressed as a proportion (%) of this total as shown in the graphs in Figs 2, 3, 4 and 5.

3D image segmentation Confocal fluorescence data were segmented with Avizo (ThermoFisher, Australia). Laminin staining identified capillaries and the islet capsule, membrane staining defined cell boundaries and insulin staining defined beta cells. A 7-pixel-wide brush was used to draw segmentation boundaries for cells, capillaries and capsules, and data were interpolated between two and seven optical slices.

Live-cell image acquisition Slice medium was replaced with Krebs Ringer bicarbonate buffer (KRBH), 2.8 mmol/l glucose, for a pre-basal period of 1 h prior to imaging. Then, 1 ml of KRBH (2.8 mmol/l glucose, 1 mmol/l sulforhodamine B [SRB] dye) was added to the microscope imaging chamber and pre-heated to 37°C. Live-cell imaging was done on a homemade multi-photon microscope with an Olympus IX71 body and a ×60 Olympus PlanApo N oil immersion objective lens. Single slices were imaged in a heat conductive, open brass chamber which held 25 mm round coverslips on a heated platform (37°C). Slices were held stationary in solution by a slice anchor (Harvard Bioscience, MA, USA).

Fluorescence was excited at 810 nm (Chameleon, Coherent Scientific, Australia) and emission captured at 6 frames per second (Photo-sensor module H7422PA-40, Hamamatsu Photonics, Hamamatsu, Japan) and visualised with Scanimage (MBF Bioscience, VT, USA) software. The SRB (peak emission 577 nm) signal was collected at >590 nm.

Exocytosis assay Data were analysed via Metamorph software (Molecular Devices, USA). Frames were manually screened to identify granule fusion events, which appear as sudden, circular flashes ~1 µm in diameter and decay over 1–3 s (3–9 frames) (Fig. 5). Once a granule fusion event had been visualised, 0.7-µm-diameter regions of interest (ROIs) were placed over the location, and granule fusion was confirmed by kymograph examination and analysed using Microsoft Excel (Microsoft 365, Microsoft, USA).

Electron microscopy Serial block face imaging (Fig. 1) was performed as previously described [5].

Statistics Data are expressed as scatter plots. Statistical analyses used GraphPad Prism 10 (Dotmatics, USA) with two-sided Student's t tests, one-way ANOVA, and Mann–Whitney and Spearman's tests where appropriate, with

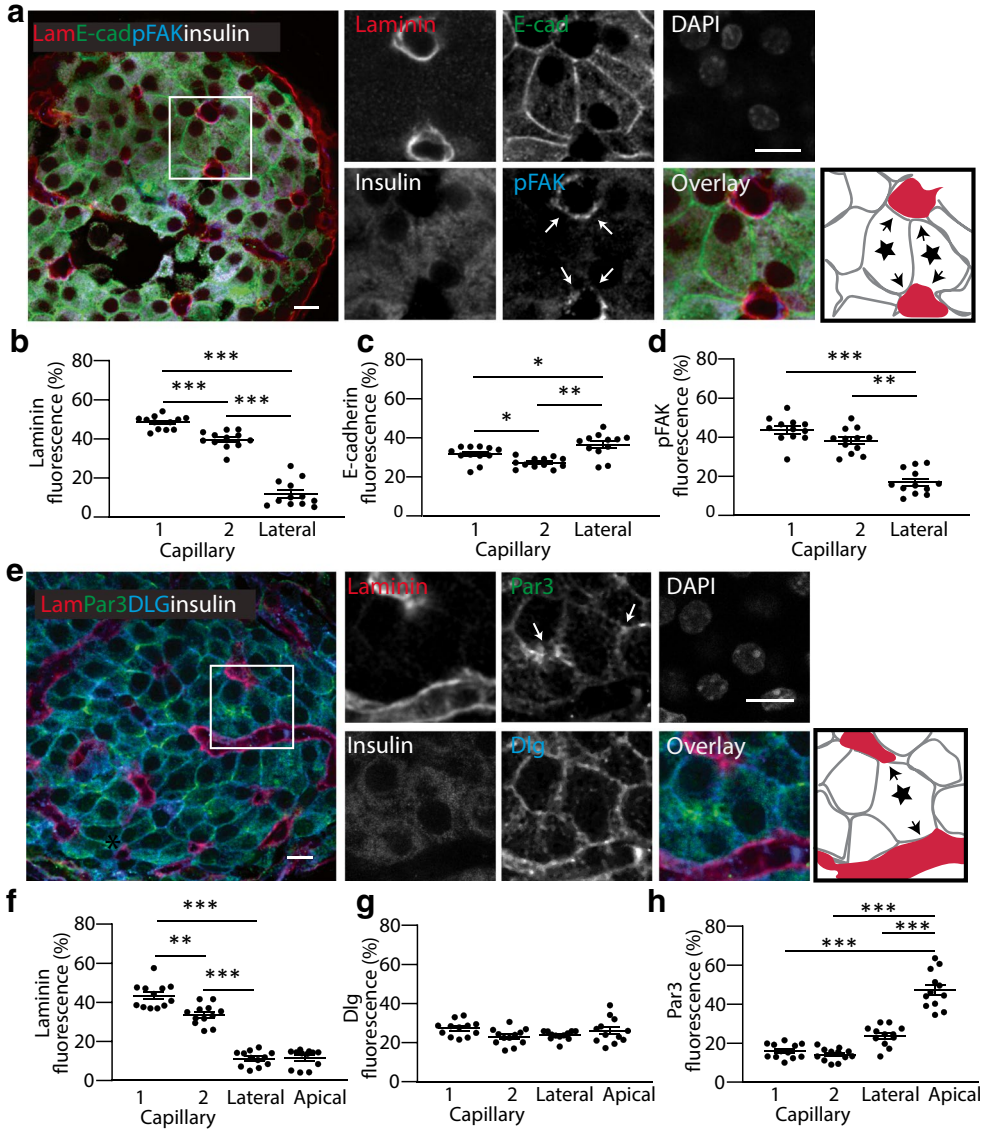

Fig. 2 In mouse islets, regional enrichment of membrane domains and segregated distribution of polarity determinants, Dlg and Par3, in cells that contact two capillaries. (**a**) Example image of the combined immunostaining of laminin (Lam), E-cadherin (E-cad) and pFAK. Enlarged images within the square ROI are shown, with arrows highlighting pFAK staining. The cartoon identifies, with stars, two beta cells with two capillary contacts (shown with arrows). (**b**) Laminin is significantly enriched at both capillary interfaces compared with the lateral surface. (**c**) E-cadherin is significantly enriched in the lateral domain compared with both capillary interfaces. (**d**) pFAK is significantly enriched at both capillary interfaces compared with the lateral surface. (**e**) Combined staining of laminin, Dlg and Par3. Enlarged images within the square ROI are shown, with arrows highlighting Par3 staining. The cartoon identifies, with a star, a beta cell with two capillary contacts (shown with arrows). (**f**) Laminin is significantly enriched at both capillary interfaces compared with the lateral and apical regions. (**g**) Dlg is found across all of the cell membrane. (**h**) Par3 is significantly enriched in the apical domain compared with lateral or capillary regions. For all data, n=12 cells from 3 mice, 4 cells each; one-way ANOVA, Tukey's multiple comparison tests and, as indicated on the graphs, *p<0.05, **p<0.01, ***p<0.001. Scale bars, 10 μm

levels of significance as indicated. Randomisation and blinding were not carried out and there were no inclusion or exclusion criteria for the samples or data. To obtain an unbiased dataset from thousands of optical sections we selected data from across at least three individuals and from multiple islets per animal, as indicated in the text.

Results

Here we use the pancreatic slice technique, for superior preservation of islet structure compared with isolated islets or paraffin sections [5, 26–28], to determine the precise relationship of beta cells with the islet capillaries.

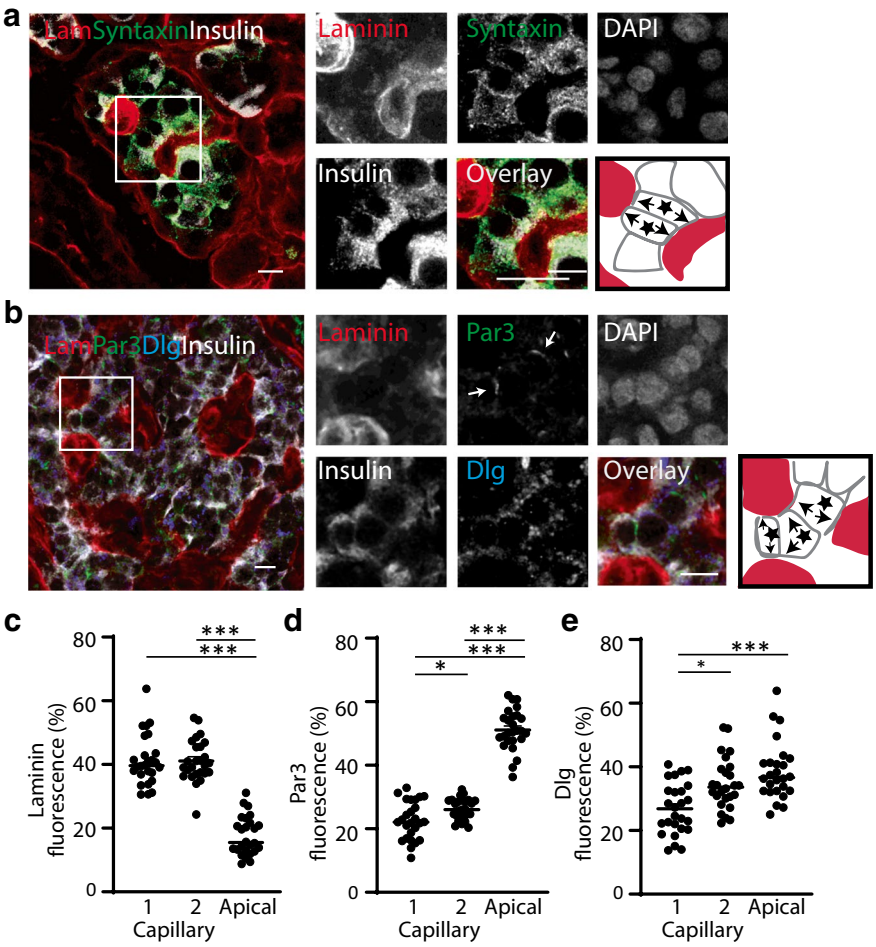

Fig. 3 In human islets, regional enrichment of polarity determinants, Dlg and Par3, in cells contacting two capillaries. (**a**) Laminin (Lam) immunostaining identifies the capillaries, insulin the beta cells and syntaxin 1A the cell outlines. The cartoon identifies, with stars, two beta cells that contact two capillaries (arrows). (**b**) Immunostaining of Par3 shows enrichment in areas away from capillary contact points (arrows highlight the Par3 staining) with Dlg staining all around the cells, including the capillary contact points. The cartoon identifies, with stars, three beta cells that contact two capillaries (arrows). (**c**) Laminin is significantly enriched at both capillary interfaces compared with the apical region. (**d**) Par3 is significantly enriched in the apical domain compared with either capillary region. (**e**) Dlg is found across all of the cell membrane. For all data, n=5 islets, 29 cells and 3 donors; one-way ANOVA, Tukey's multiple comparison tests and, as indicated on the graphs, *p<0.05, ***p<0.001. Scale bars, 10 µm

With fixed-cell immunofluorescence in mouse and human islets, we collected hundreds of serial optical sections through the islets. Immunostaining of laminin marked the capillaries. Laminin is an ECM protein exclusively secreted by capillary wall cells [15]. We counter immunostained for insulin to identify beta cells and for epithelial cadherin (E-cadherin), a cell junction protein, to outline the cells (Fig. 1a). We assessed, in three-dimensions for each cell, the number of capillary contacts, showing most mouse beta cells have one capillary contact but ~30% have two (Fig. 1b). Multiple points of capillary contact were also seen in serial electron micrograph sections (Fig. 1c,d). Furthermore, analysis of human islets also showed a significant proportion of beta cells with two points of capillary contact (Fig. 1e).

Structural organisation of beta cells with multiple capillary contacts The canonical organisation of polarised epithelia is one basal pole, a lateral domain and one apical pole [17]. For beta cells with one point of capillary contact there is a similar organisation [5, 17]. Here we set out to determine the effect of contact with two capillaries on beta cell polarity.

We used immunofluorescence in mouse islets for laminin and E-cadherin, as in Fig. 1, and in addition stained for phosphorylated focal adhesion kinase (pFAK) which is a component of the integrin response (Fig. 2a). Fluorescence intensities showed, as expected, laminin enrichment at both capillary contacts and absence in the lateral domain (Fig. 2b,f). E-cadherin was enriched in the lateral domain, with some evidence for presence at the capillary interface (Fig. 2c). pFAK was enriched at both capillary interfaces, demonstrating an integrin response at each of the ECM contacts (Fig. 2d). We next studied the distribution of the polarity determinant proteins, discs large (Dlg) (basal) and partitioning defective protein 3 (Par3) (apical/junctional), in cells that contacted two capillaries (Fig. 2e). Dlg was present across all membranes (Fig. 2g) and Par3 was located away from both capillary interfaces, indicating enrichment in a putative apical domain (Fig. 2h).

Immunostaining of human islets showed a similar organisation to mouse beta cells. In our hands the E-cadherin antibody gave poor staining in human islets, and therefore to outline the beta cells we stained for syntaxin 1A, which

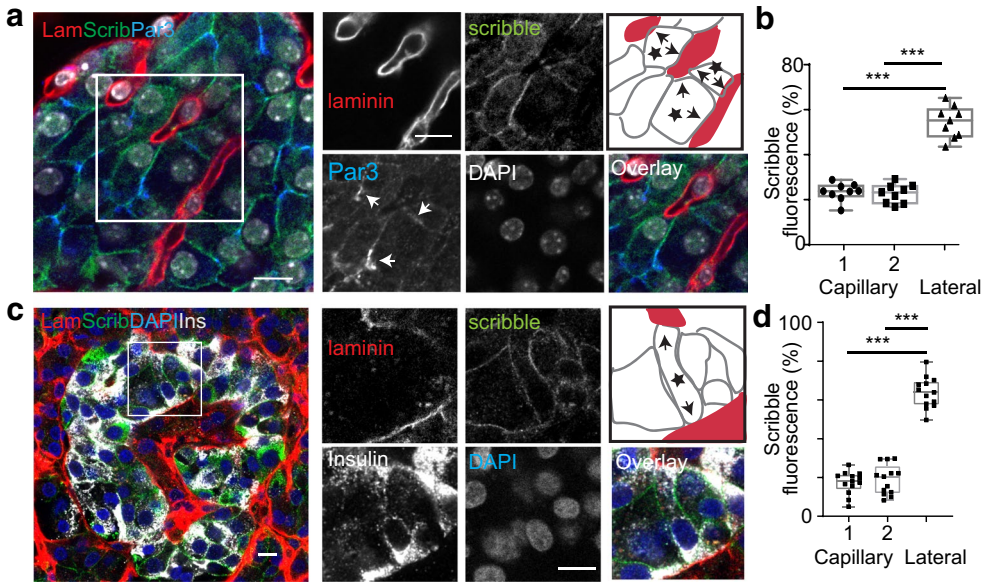

Fig. 4 In mouse and human islets, regional localisation of the basolateral determinant scribble with cells that contact two capillaries. (**a**, **b**) In mouse islets, for beta cells that contact two capillaries, scribble is across all of the membrane but enriched at the lateral membrane. The cartoon identifies, with stars, three beta cells that contact two capillaries (arrows). Par3, the apical/junctional polarity determinant, is located away from the capillaries (arrows highlight the Par3 staining). Analysis of ROIs shows significant enrichment of scribble at the lateral membrane (n=9 cells; one-way ANOVA, Tukey's multiple comparison tests, capillary 1/capillary 2 p=0.89 and, as indicated on the graphs, ***p<0.001). (**c**, **d**) In human islets, scribble shows a similar localisation to mouse and is present across all of the membrane, with enrichment at the lateral sides of the cells. The cartoon identifies, with a star, a beta cell that contacts two capillaries (arrows). Analysis of ROIs showed scribble was significantly enriched on the lateral surfaces (n=13 cells, 4 islets, 2 donors; one-way ANOVA, Tukey's multiple comparison tests, capillary 1/capillary 2 p=0.86 and, as indicated on the graphs, ***p<0.001). Scale bars, 10 µm. Ins, insulin; Lam, laminin; Scrib, scribble

is enriched across all of the membrane (Fig. 3a) [10]. We used Par3 and Dlg immunostaining, which showed Par3 was enriched away from the capillaries and Dlg was present across all of the membrane (Fig. 3b–e). Further immunolabelling (Fig. 4) for the basolateral determinant scribble, which is a protein associated with cadherin junctions in epithelial cells, showed, in both mouse (Fig. 4a,b) and human (Fig. 4c,d) islets, that it was present across all of the beta cell membrane.

We conclude that in beta cells with two capillary contacts, a distinct form of polarisation develops with multiple basal domains.

Both capillary contacts in beta cells are enriched in proteins specialised to regulate secretion One functional consequence of ECM contact is to localise insulin secretion [29] through local activation of integrins [9] and local enhancement of the calcium response [11, 28]. We therefore tested whether both capillary contact points are specialised for secretion.

We used immunofluorescence for the presynaptic scaffold proteins, liprin and ELKS [30], which are important in controlling insulin secretion [11, 12]. In mouse islets, liprin (Fig. 5a,b) and ELKS (Fig. 5c,d) were significantly and equally enriched in beta cells at both capillary contacts. A similar enrichment of liprin was found at both capillary contact points in human beta cells (Fig. 5e,f). These results demonstrate that both capillary contacts in beta cells are enriched in synaptic scaffold proteins and potentially specialised for secretion.

Both capillary contacts in beta cells are targets for insulin granule fusion To identify the significance on secretion, we used live-cell experiments with an extracellular fluid-phase marker to record granule fusion events. Each individual fusion event is observed as a sudden increase in fluorescence as the extracellular dye enters the fusing granule, which decays over time as the granule collapses into the cell membrane (see Fig. 6a) [31]. We have shown this fluorescence signature co-localises with immunostained insulin and overlaps with the efflux of expressed proinsulin-GFP [32], giving us an indirect method for determining insulin granule fusion events in space and time [10, 28, 31].

Mouse pancreatic slices were stimulated for 20 min with 16.7 mmol/l glucose plus 10 µmol/l forskolin (Fig. 6b). Each individual fusion event is marked with a yellow dot, enabling us to map out the cumulative spatial pattern of granule fusion over the 20 min of stimulation (Fig. 6b). In this example, three cells each contact two capillaries (Fig. 6b).

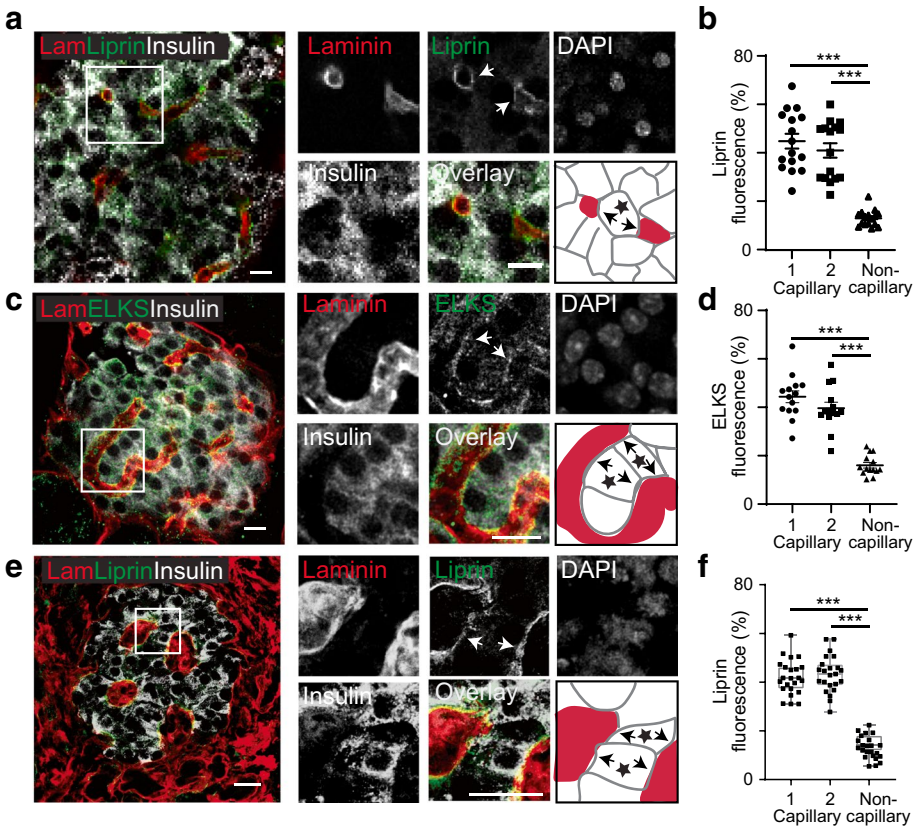

Fig. 5 In mouse and human islets, beta cells that make two points of capillary contact show presynaptic scaffold proteins are enriched at both contact points. (**a**) In mouse islets, the immunostaining of laminin (Lam) identifies the capillaries and insulin the beta cells. Immunostaining of the presynaptic scaffold protein liprin α1 showed enrichment at both the capillary interfaces. The cartoon identifies, with a star, a beta cell with two capillary contacts. (**b**) Analysis of fluorescence intensity within ROIs shows significant liprin enrichment at the capillaries (n=16 cells, 4 islets, 3 mice; ANOVA, Tukey's multiple comparisons, capillary 1/capillary 2 p=0.79 and, as indicated on the graphs, ***p<0.001). (**c**) In mouse islets, another presynaptic scaffold protein, ELKS, also showed enrichment at both the capillary interfaces. The cartoon identifies, with stars, two beta cells with two capillary contacts. (**d**) Analysis of fluorescence intensity within ROIs shows significant ELKS enrichment at the capillaries (n=14 cells, 5 islets, 5 mice; ANOVA, Tukey's multiple comparisons, capillary 1/capillary 2 p=0.59 and, as indicated on the graphs, ***p<0.001). (**e**) In human islets we observed a similar enrichment of liprin α1 at the capillary interface. The cartoon identifies, with stars, two beta cells with two capillary contacts. (**f**) Analysis of fluorescence intensity within ROIs shows significant liprin enrichment at the capillaries (n=23 cells, 7 islets, 3 donors; ANOVA, Tukey's multiple comparisons, capillary 1/capillary 2 p=0.59 and, as indicated on the graphs, ***p<0.001). Scale bars, 10 µm for the mouse islets and 20 µm for human

Analysis shows that both capillary contacts are the target for granule fusion (Fig. 6b,c).

We conclude that in beta cells with two capillary contacts, both contacts support exocytosis and are functionally equivalent for secretion.

Granule fusion at the capillary contacts can be differentially controlled Past work on beta cells with one point of capillary contact shows this contact is the target for granule fusion [28], local enhancement of the calcium response [11, 28] and enrichment of synaptic scaffold proteins [10]. This has led to the proposal that the capillary interface of beta cells has a presynaptic-like organisation that locally regulates secretion [33]. If this is the case, then the two points of contact might function somewhat independently of each other due to locally different regulation or structures.

To test this, mouse pancreatic slices were stimulated with glucose (16.7 mmol/l) and forskolin (10 µmol/l) for 20 min and exocytic events recorded as before in space (Fig. 7a,c) and now in time over the period of stimulation (Fig. 7b,d). Interestingly, the temporal patterns of granule fusion events per 60 s time bin were different for each of the capillary contact regions. When this difference was plotted out over time, it appeared that the biggest difference occurred at the earlier time points (Fig. 7f). A Spearman correlation analysis of the occurrence of fusion events at each contact in each time bin showed no significant correlation in 10/12 cells. The two cells with significant correlations (p<0.05) both had a positive correlation (r_s=0.51 and 0.55), indicating fusion events at each contact point were coordinated (an example cell is shown in Fig. 7e).

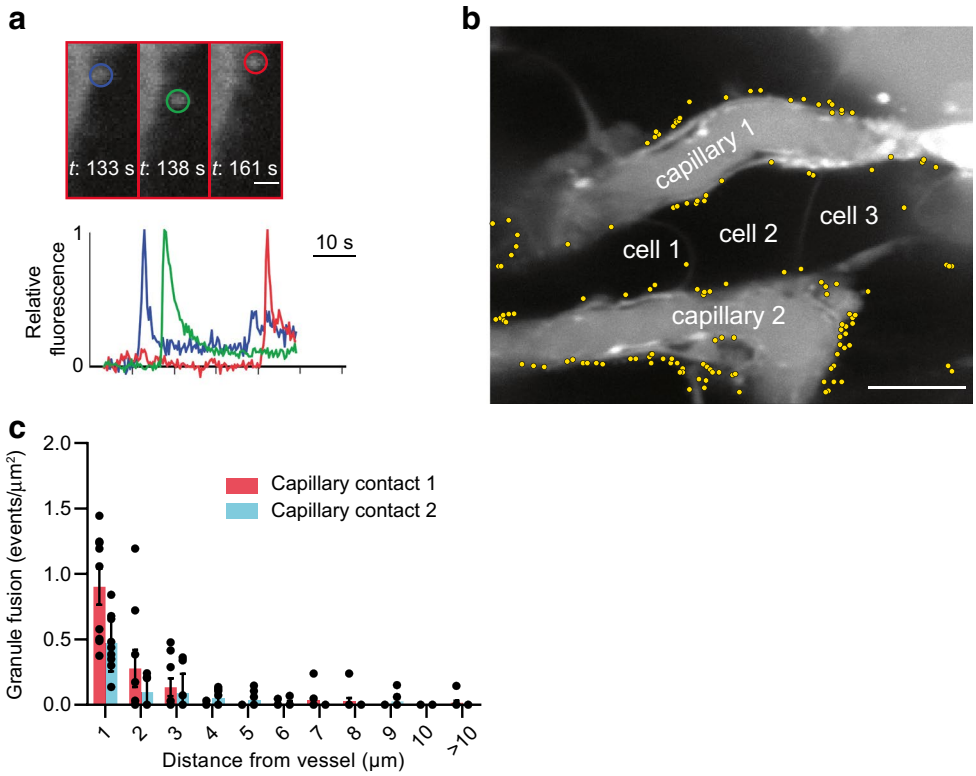

Fig. 6 Glucose-dependent granule fusion is targeted to both points of capillary contact. (**a**) In live pancreatic slices, stimulated with high glucose (16.7 mmol/l) and forskolin (10 μmol/l), granule fusion events are transiently labelled by the sudden influx of extracellular dye, SRB, into the granule. In this example image, three granule fusion events (identified by coloured circles) occurred at different times but within proximity, and plotting the fluorescence changes over time shows the characteristic peak and decay of fluorescence as the granules fuse. Scale bar, 1 μm. (**b**) Measured over 20 min of high glucose and forskolin stimulation, the location of each identified granule fusion event is shown as a yellow dot. The distribution of granule fusion events in cells that contact two capillaries (capillary 1 and capillary 2, identified by the extracellular dye) is strongly enriched at both contact points. Scale bar, 10 μm. (**c**) The frequency of granule fusion events in each cell, per length of capillary, was significantly clustered towards the capillaries (Wilcoxon matched pairs signed rank test comparing <1 μm away with >1 μm away, $p<0.05$). However, the number of fusion events at, or close to, one capillary was the same as the other capillary ($n=9$ cells, 5 islets and 3 mice; Wilcoxon matched pairs signed rank test, $p=0.10$). *t*, time

These data demonstrate that granule exocytosis at each capillary contact can be differentially controlled, providing further evidence for very local, presynaptic-like control of granule fusion.

Greater capillary contact area is linked to more insulin secretion We next compared secretion from beta cells with one capillary contact with secretion from those with two. We reanalysed our data to determine the total number of granule fusion events in each cell (note, this is the number of events per cell within the optical slice). The results show significantly more granule fusion events in the cells with two contacts, compared with cells with one (Fig. 8a). However, the surface area of contact with capillaries, as measured by pFAK staining area, was also significantly greater for cells with two contacts (Fig. 8b). When normalised against contact area there was no difference in granule fusion density between cells with one or two capillary contacts (Fig. 8c), suggesting that the underlying mechanisms that control granule fusion are similar in both cell populations. Furthermore, the plot, for each cell, of the total area of capillary contact, against the total number of granule fusion events, is linearly related (linear regression, $p<0.001$), with overlap in the distributions for cells with one or two capillary contacts (Fig. 8d).

These findings lead to an interesting possibility that overall islet secretory output is determined by the sum of the total contact area of all the beta cells with the capillaries.

Type two diabetes and changes in capillary structure In terms of disease, islet capillary structure changes in type two diabetes, described as a decrease in capillaries in rodents [19, 23] or an increase in humans [20]. In the light of our findings, we wanted to determine whether changes in capillary structure affect the beta cell contacts using the *db*/*db* mouse model of type 2 diabetes. To analyse the 3D data, we segmented the images to define the capillaries (with laminin) and a subset of beta cells (with insulin and E-cadherin). We found changes in

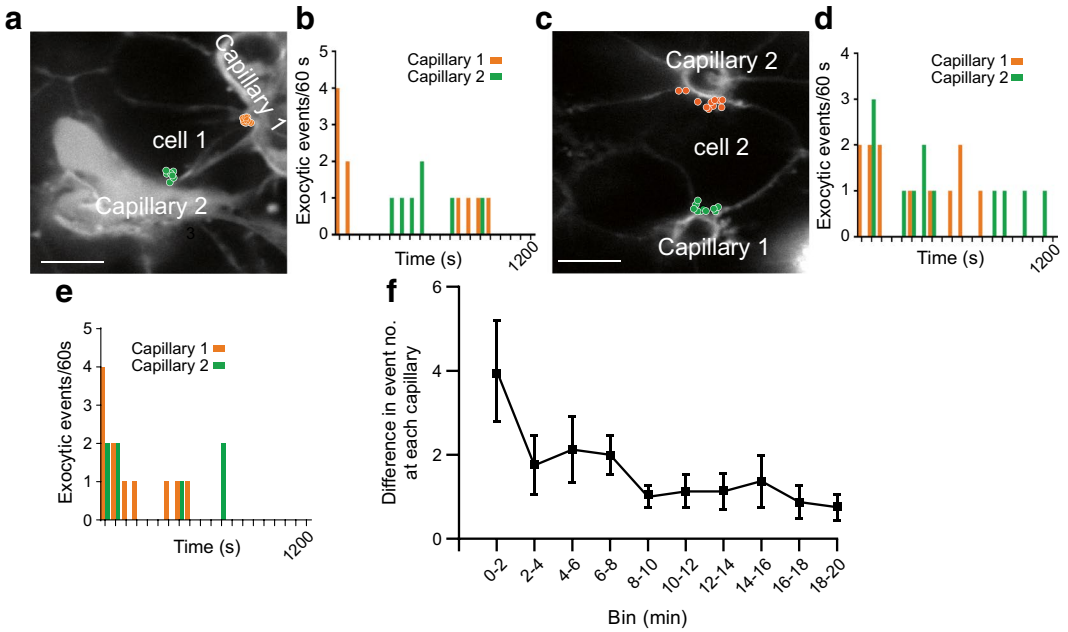

Fig. 7 Exocytic event timing is different at each capillary contact point. Granule fusion events induced by high glucose (16.7 mmol/l) and forskolin (10 μmol/l) for 20 min were identified. (**a**) Exocytic events in one cell contacting two capillaries are identified in space by the coloured circles. (**b**) The same data as in (**a**) showing the timing of each fusion event (in 60 s bins) during glucose stimulation. Analysis of this example showed no significant correlation between the occurrences of fusion events in one capillary vs the other (Spearman's correlation analysis r_s=−0.22, p=0.35). (**c**, **d**) Another example response to glucose. Analysis again showed no significant correlation between the occurrences of fusion events in one capillary vs the other (Spearman's correlation analysis r_s=−0.09, p=0.69). (**e**) An example where the occurrence of fusion events in one capillary was correlated with the other (Spearman's correlation analysis r_s=0.51, p<0.05). (**f**) Plots of the difference in fusion event numbers between each capillary contact, per time bin, show the biggest difference at the beginning of glucose stimulation (n=9 cells, 5 islets, 3 mice). Scale bars, 5 μm

capillary shape in disease, as shown with the immunostaining (Fig. 9a,b) and in the segmented images (Fig. 9c,d). Determination of the proportion of cells that make one or two capillary contacts, using serial immunofluorescence images, showed an almost complete loss of cells with two capillary contacts (Fig. 9e) and an increase in cells with no apparent contacts (compare Fig. 1b with Fig. 9e). Relative to islet size, analyses of the segmented data showed that the volume of capillaries does not change (Fig. 9f); however, there was a significant decrease in the capillary surface area (Fig. 9g). Analysis of the segmented data for beta cell contacts showed that this change in capillary structure reduced the overall contact area of each beta cell with the capillary (Fig. 9h).

We conclude that the diabetes-induced changes in islet capillary structure do impact the relationship with beta cells and decrease the beta cell contact area with the capillary ECM.

Discussion

We identify that 36% of mouse and 22% of human beta cells contact two capillaries. These cells have an unusual form of cell polarity, with a basal domain at each contact and an apical domain away from the capillaries (Figs 2, 3 and 4). Each capillary contact is enriched in synaptic scaffold proteins and is a target for insulin granule fusion (Figs 5, 6 and 7). Intriguingly, the contact points can function independently, indicating very local control of secretion (Fig. 7). Independent of the number of capillary contacts made by a beta cell, increased insulin secretion is correlated with increased capillary contact area (Fig. 8d).

In the *db*/*db* mouse model of diabetes, we observe that the total capillary volume per islet is unchanged, but there is a significant reduction both in capillary surface area per islet and in the area of capillary contact per individual beta cell, and an almost complete loss of cells with two capillary contacts (Fig. 9). These changes could contribute to the reduced secretion in disease and to disease progression.

These insights identify the beta cell to capillary contacts as a new factor defining beta cell polarity, regulating insulin secretion and undergoing significant changes in disease.

Is this a distinct subpopulation of beta cells? Heterogeneity across beta cells within an islet includes mature vs immature beta cells [34], functional distinctions that lead to distinct cell responses [35] and markers for different cell subtypes [36]. We have segregated beta cells into two populations

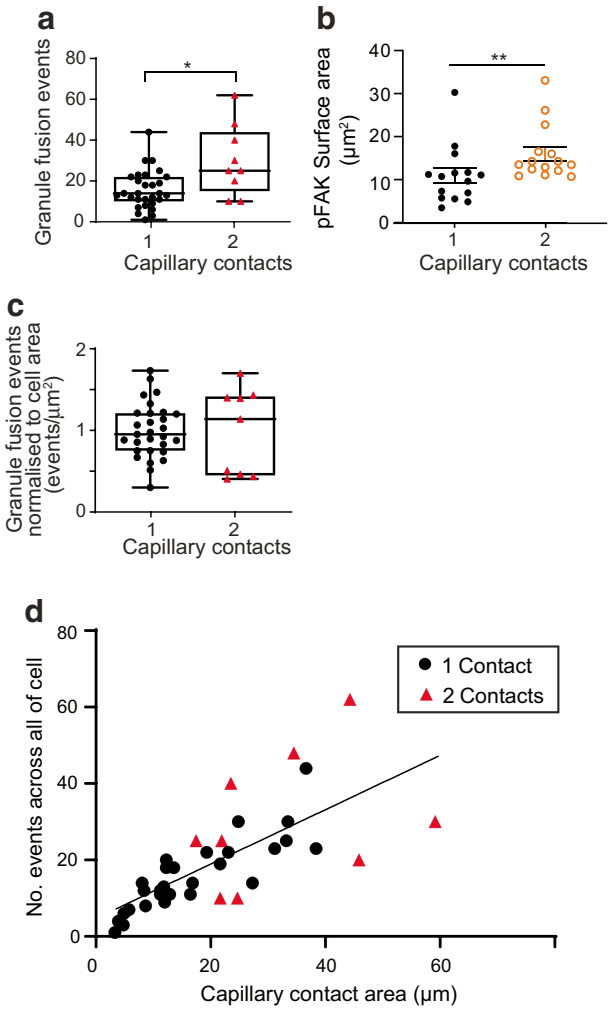

Fig. 8 Beta cells with two capillary contacts have more insulin granule fusion events. (**a**) The total number of granule fusion events per cell in response to 16.7 mmol/l glucose and 10 μmol/l forskolin for 20 min was significantly greater for cells making contact with two capillaries than for cells making contact with one capillary (n=38 cells, 5 islets, 3 mice; Mann–Whitney test, *p<0.05). (**b**) The pFAK surface area was significantly larger in beta cells making contact with two capillaries than in cells making contact with one capillary (n=15 cells, 3 islets, 3 mice; Mann–Whitney test, **p<0.01). (**c**) The granule fusion data now normalised for cell surface area show no difference in the number of granule fusion events per μm^2 (n=38 cells, 5 islets, 3 mice; Mann–Whitney test, p=0.92). (**d**) A plot of total granule fusion events per cell plotted against total capillary area per cell approximated to a linear relationship, with cells contacting one capillary (circles) intermixed with cells contacting two capillaries (red triangles) (n=38 cells, 5 islets, 3 mice; line fitted to all data points with a slope of 0.71, R^2 0.52, significant, p<0.001)

based on an anatomical distinction and show an impact on cell polarity and insulin secretion. In this way, the beta cells with two capillary contacts are distinct: they have a different form of polarity and the larger area of contact with capillaries drives bigger responses to glucose.

The beta cell capillary interface as a key factor in controlling insulin secretion Our data show most beta cells contact two obviously separate capillaries, but we cannot exclude that sometimes the same capillary makes both contacts. This could be important if populations of capillaries of the islet were segregated into distinct functions and reminds us of arguments around whether there is a systematic blood flow through the islet (e.g. core to periphery) [37]. The most recent data show no specialised flow [18, 38] and instead indicate an interleaving of islet capillaries with the surrounding acinar tissue [18]. This does not exclude the idea of specialised capillaries but is consistent with the similar function we show for both capillary contacts.

Our conclusion that beta cell capillary contact area is a key driver for insulin secretion is new but is consistent with past work. ECM proteins enhance beta cell proliferation and secretion [29, 39] and one route for these effects is through integrin and focal adhesion kinase (FAK) activation [9, 28, 29]. What is new here is that the contact area for each cell appears to be a limiting factor for insulin secretion: the greater the contact area, the greater the secretion. It should be noted that the data that support this idea (Fig. 8) are analyses of two-photon data (Fig. 6). These experiments count the number of exocytic events just in that optical plane and not across the whole cell. However, the correlation we see (Fig. 8d) and the data overlap between cells with one and two capillary contacts (Fig. 8c) is strong evidence that contact area alone is a limiting step in granule fusion.

The limiting factor(s) could be structural, such as limited access of granules to the cell membrane, or a signalling factor, such as localised calcium entry. It is intriguing that we now show that the two contact points have evidence for independent function. This suggests local control, at the contact points, of key elements of the stimulus–secretion cascade. This idea is supported by work showing local enhanced calcium responses at the capillary interface [11, 28] and that sites of insulin granule fusion are enriched in proteins that control exocytosis [40].

Broader relevance of our findings Our work uses pancreatic slices, where islet structure is well preserved, and, by comparison with isolated islets, slices have fast calcium waves and enhanced glucose-dependent insulin secretion [28]. The slice therefore represents an excellent in vitro system. However, both external innervation and blood flow are lost in slices and both these factors might influence beta cell biology [41]. Notwithstanding these drawbacks, the slice is an important tool for understanding islet biology and is a considerable advance on the use of isolated islets.

It is important to note that we focus on the response of beta cells to the capillary ECM [15]. However, beta cell function is also influenced by other interactions with capillary cells, including endothelial cells [21, 42] and pericytes,

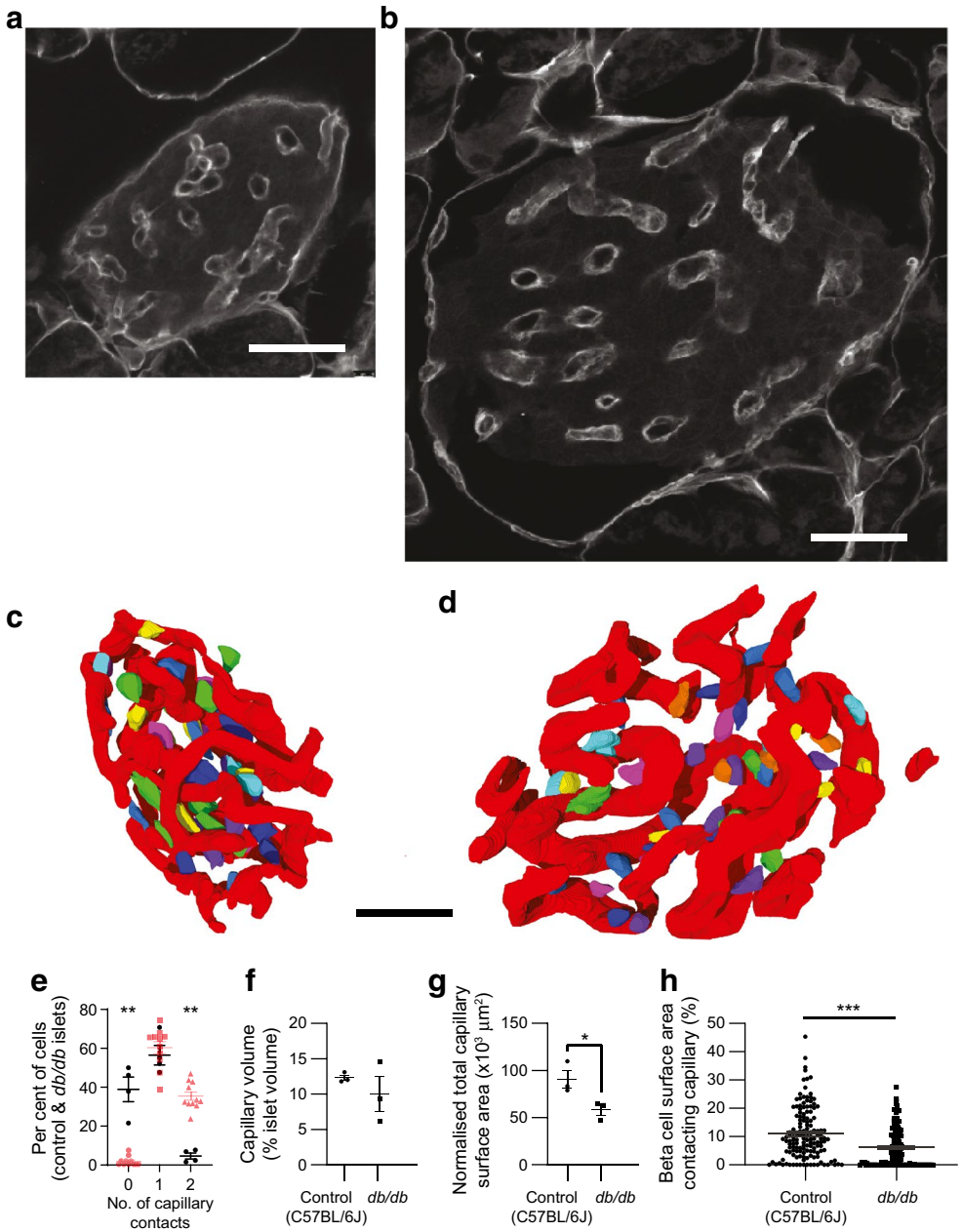

Fig. 9 Capillary structure changes in the *db*/*db* mouse model of diabetes impact on beta cell capillary contacts. (**a**) A control islet immunostained with laminin and (**b**) an islet from a *db*/*db* mouse stained with laminin show enlargement of the islet and changes to capillary structure. (**c**) Control and (**d**) *db*/*db* islets show segmentation of confocal image stacks outlining the 3D capillary structure (red) and the relationship with a randomly selected set of beta cells (multiple colours) within the islet. (**e**) The proportion of cells contacting zero, one or two capillaries was estimated using serial sectioning (as in Fig. 1, n=4 *db*/*db* islets from 3 mice). For comparison, the red symbols are the same data as in Fig. 1b from C57 control mice. Mann–Whitney tests showed significant differences between control and *db*/*db* islets in the numbers with zero (**p<0.01) and two (**p<0.01) contacts but not with one contact (p=0.49). (**f**) Analysis of the segmented images showed no difference in total capillary volume expressed as a proportion of total islet volume in *db*/*db* islets compared with control islets (n=3 control islets and 3 *db*/*db* islets, each from 3 mice; two-sided Student's t test, p=0.41). (**g**) However, capillary complexity was reduced in *db*/*db* islets and this was identified as a decrease in the total capillary surface area, normalised to total islet volume (n=3 control islets and 3 *db*/*db* islets, each from 3 mice; two-sided Student's t test, *p<0.05). (**h**) The capillary contact area per beta cell was reduced in *db*/*db* islets (n=294 cells, 6 islets, 6 mice; two-sided Student's t test, ***p<0.001). Scale bars, 50 µm

which affect beta cell maturation and function [43] and alter islet blood flow [44] to regulate insulin secretion [45].

Impact of islet vascular changes in type 2 diabetes A defining characteristic of type 2 diabetes is changes to the systemic capillary network [46, 47]. In islets, changes to capillaries have been observed but are difficult to define [20–22, 48] because of the complexity of the volumes and changes in the overall size and structure of the islet which alter over the progression of the disease [24, 49]. However, our work clearly identifies a common factor in diseased islets. The islets we studied were from mice with overt diabetes where capillaries got bigger with less complexity, measured in terms of a reduction in capillary surface area per islet volume. This result is reinforced with measurements on single cells which show a significant reduction in percentage area of capillary contact (Fig. 9).

We speculate that our findings identify a novel vicious cycle that propels disease progression. In early disease, changes in cell signalling and compensatory increases in islet beta cell mass [49] might be paralleled with changes in capillaries to preserve beta cell capillary contact area and secretory output. However, as disease progresses hyperglycaemia damages capillary structure which decreases beta cell capillary contact area and leads to a consequent reduction in insulin secretion, further accelerating loss of glucose homeostasis. This might be compounded by the glucotoxic damage and loss of beta cells in diabetes which would be expected to reduce vascular endothelial growth factor A (VEGFA) secretion from beta cells [50, 51], which is a known driver of islet vascularisation.

Supplementary Information The online version contains peer-reviewed but unedited supplementary material available at https://doi.org/10.1007/s00125-024-06180-x.

Acknowledgements We thank all organ donors, participants and their families for their generosity and for enabling this work. We also thank the staff of St Vincent's Institute involved in the islet isolation programme and Donatelife for obtaining research consent and providing the human pancreases. Some samples used in the work were obtained through the Network for Pancreatic Organ donors with Diabetes (nPOD). This research was performed with the support of nPOD (RRID:SCR_014641), a collaborative type 1 diabetes research project sponsored by JDRF (nPOD: 5-SRA-2018-557-Q-R) and The Leona M. & Harry B. Helmsley Charitable Trust (grant no. 2018PG-T1D053). The content and views expressed are the responsibility of the authors and do not necessarily reflect the official view of nPOD. Organ Procurement Organisations (OPOs) partnering with nPOD to provide research resources are listed at http://www.jdrfnpod.org/for-partners/npod-partners/. Imaging was performed in the Centre for Microscopy and Microanalysis at the University of Sydney, and we thank the staff for their support of this project. We thank C. Ludick and K. Sun (University of Sydney) for input into the analysis of data. We thank the electron microscopy team of R. Parton, Robyn Webb and Richard Webb (University of Queensland) for the acquisition of the original data used in Fig. 1.

Data availability All data generated or analysed during this study are included in the article. No additional resources were generated or analysed during the current study.

Funding Open Access funding enabled and organized by CAUL and its Member Institutions. This project was funded by the NHMRC (grant no. APP1146788 to PT and JSS, grant no. APP1128273 to PT) and Diabetes Australia (grant no. DART Y18G_THOP to PT).

Authors' relationships and activities The authors declare that there are no relationships or activities that might bias, or be perceived to bias, their work.

Contribution statement DJ and LC made substantial contributions to conception and design, acquisition of data, analysis and interpretation of data. NH made substantial contributions to the experimental design and the acquisition of data. JSS, AJG, TL, HET and RH all made contributions to the conception of the project and acquisition of material and data. PT made substantial contributions to conception and design, analysis and interpretation of data. All authors contributed to drafting the article or revising it critically for important intellectual content and have given final approval of the version to be published. PT is the guarantor of this work and, as such, had full access to all the data in the study and takes responsibility for the integrity of the data and the accuracy of the data analysis.

References

1. Lombardi T, Montesano R, Wohlwend A, Amherdt M, Vassalli J-D, Orci L (1985) Evidence for polarization of plasma membrane domains in pancreatic endocrine cells. Nature 313(6004):694–696. https://doi.org/10.1038/313694a0
2. Bonner-Weir S (1988) Morphological evidence for pancreatic polarity of beta cell within islets of Langerhans. Diabetes 37:616–621. https://doi.org/10.2337/diab.37.5.616
3. Lucocq J, Montesano R (1985) Nonrandom positioning of Golgi apparatus in pancreatic B cells. Anat Rec 213(2):182–186. https://doi.org/10.1002/ar.1092130210
4. Granot Z, Swisa A, Magenheim J et al (2009) LKB1 regulates pancreatic beta cell size, polarity, and function. Cell Metab 10(4):296–308. https://doi.org/10.1016/j.cmet.2009.08.010
5. Gan WJ, Zavortink M, Ludick C et al (2017) Cell polarity defines three distinct domains in pancreatic beta-cells. J Cell Sci 130:143–151. https://doi.org/10.1242/jcs.185116
6. Orci L, Thorens B, Ravazzola M, Lodish HF (1989) Localization of the pancreatic beta cell glucose transporter to specific plasma membrane domains. Science 245(4915):295–297. https://doi.org/10.1126/science.2665080
7. Farack L, Golan M, Egozi A et al (2019) Transcriptional heterogeneity of beta cells in the intact pancreas. Dev Cell 48(1):115-125.e114. https://doi.org/10.1016/j.devcel.2018.11.001

8. Hughes JW, Cho JH, Conway HE et al (2020) Primary cilia control glucose homeostasis via islet paracrine interactions. Proc Natl Acad Sci U S A 117(16):8912–8923. https://doi.org/10.1073/pnas.2001936117
9. Gan WJ, Do OH, Cottle L et al (2018) Local integrin activation in pancreatic β cells targets insulin secretion to the vasculature. Cell Reports 24(11):2819-2826.e2813. https://doi.org/10.1016/j.celrep.2018.08.035
10. Low JT, Zavortink M, Mitchell JM et al (2014) Insulin secretion from beta cells in intact mouse islets is targeted towards the vasculature. Diabetologia 57(8):1655–1663. https://doi.org/10.1007/s00125-014-3252-6
11. Ohara-Imaizumi M, Aoyagi K, Yamauchi H et al (2019) ELKS/voltage-dependent ca($^{2+}$) channel-beta subunit module regulates polarized ca($^{2+}$) influx in pancreatic beta cells. Cell Reports 26(5):1213–1226. https://doi.org/10.1016/j.celrep.2018.12.106
12. Ohara-Imaizumi M, Ohtsuka T, Matsushima S et al (2005) ELKS, a protein structurally related to the active zoneassociated protein CAST, is expressed in pancreatic beta cells and functions in insulin exocytosis: Interaction of ELKS with exocytotic machinery analyzed by total internal reflection fluorescence microsscopy. Mol Biol Cell 16(7):3289–3300. https://doi.org/10.1091/mbc.E04-09-0816
13. Yasuda T, Shibasaki T, Minami K et al (2010) Rim2 alpha determines docking and priming states in insulin granule exocytosis. Cell Metab 12(2):117–129. https://doi.org/10.1016/j.cmet.2010.05.017
14. Fujimoto K, Shibasaki T, Yokoi N et al (2002) Piccolo, a Ca^{2+} sensor in pancreatic beta-cells - Involvement of cAMP-GEFII center dot Rim2 center dot Piccolo complex in cAMP-dependent exocytosis. J Biol Chem 277(52):50497–50502. https://doi.org/10.1074/jbc.M210146200
15. Nikolova G, Jabs N, Konstantinova I et al (2006) The vascular basement membrane: a niche for insulin gene expression and beta cell proliferation. Dev Cell 10(3):397–405. https://doi.org/10.1016/j.devcel.2006.01.015
16. Lammert E, Thorn P (2020) The role of the islet niche on beta cell structure and function. J Mol Biol 432(5):1407–1418. https://doi.org/10.1016/j.jmb.2019.10.032
17. Bryant DM, Roignot J, Datta A et al (2014) A molecular switch for the orientation of epithelial cell polarization. Dev Cell 31(2):171–187. https://doi.org/10.1016/j.devcel.2014.08.027
18. Dybala MP, Kuznetsov A, Motobu M et al (2020) Integrated pancreatic blood flow: bidirectional microcirculation between endocrine and exocrine pancreas. Diabetes 69(7):1439–1450. https://doi.org/10.2337/db19-1034
19. Mizuno A, Noma Y, Kuwajima M, Murakami T, Zhu M, Shima K (1999) Changes in islet capillary angioarchitecture coincide with impaired B-cell function but not with insulin resistance in male Otsuka-Long-Evans-Tokushima fatty rats: dimorphism of the diabetic phenotype at an advanced age. Metabolism 48(4):477–483. https://doi.org/10.1016/S0026-0495(99)90107-5
20. Brissova M, Shostak A, Fligner CL et al (2015) Human islets have fewer blood vessels than mouse islets and the density of islet vascular structures is increased in type 2 diabetes. J Histochem Cytochem 63(8):637–645. https://doi.org/10.1369/0022155415573324
21. Hogan MF, Liu AW, Peters MJ et al (2016) Markers of Islet endothelial dysfunction occur in male B6.BKS(D)-Leprdb/J mice and may contribute to reduced insulin release. Endocrinology 158(2):293–303. https://doi.org/10.1210/en.2016-1393
22. Dai C, Brissova M, Reinert RB et al (2013) Pancreatic islet vasculature adapts to insulin resistance through dilation and not angiogenesis. Diabetes 62(12):4144–4153. https://doi.org/10.2337/db12-1657
23. Nakamura M, Kitamura H, Konishi S et al (1995) The endocrine pancreas of spontaneously diabetic db/db mice: microangiopathy as revealed by transmission electron microscopy. Diabetes Res Clin Pract 30(2):89–100. https://doi.org/10.1016/0168-8227(95)01155-2
24. Do OH, Gunton JE, Gaisano HY, Thorn P (2016) Changes in beta cell function occur in prediabetes and early disease in the Lepr mouse model of diabetes. Diabetologia 59:1222–1230. https://doi.org/10.1007/s00125-016-3942-3
25. Schindelin J, Arganda-Carreras I, Frise E et al (2012) Fiji: an open-source platform for biological-image analysis. Nat Methods 9(7):676–682. https://doi.org/10.1038/nmeth.2019
26. Lukinius A, Jansson L, Korsgren O (1995) Ultrastructural evidence for blood microvessels devoid of an endothelial-cell lining in transplanted pancreatic-islets. Am J Pathol 146(2):429–435
27. Cottle L, Gan WJ, Gilroy I et al (2021) Structural and functional polarisation of human pancreatic beta cells in islets from organ donors with and without type 2 diabetes. Diabetologia 64:618–629. https://doi.org/10.1007/s00125-020-05345-8
28. Jevon D, Deng K, Hallahan N et al (2022) Local activation of focal adhesion kinase orchestrates the positioning of presynaptic scaffold proteins and Ca^{2+} signalling to control glucose-dependent insulin secretion. eLife 11:e76262. https://doi.org/10.7554/eLife.76262
29. Rondas D, Tomas A, Halban PA (2011) Focal adhesion remodeling is crucial for glucose-stimulated insulin secretion and involves activation of focal adhesion kinase and paxillin. Diabetes 60(4):1146–1157. https://doi.org/10.2337/db10-0946
30. Sudhof TC (2012) The presynaptic active zone. Neuron 75(1):11–25. https://doi.org/10.1016/j.neuron.2012.06.012
31. Low JT, Mitchell JM, Do OH et al (2013) Glucose principally regulates insulin secretion in islets by controlling the numbers of granule fusion events per cell. Diabetologia 56(12):2629–2637. https://doi.org/10.1007/s00125-013-3019-5
32. Ma W, Chang J, Tong J et al (2020) Arp2/3 nucleates F-actin coating of fusing insulin granules in pancreatic beta cells to control insulin secretion. J Cell Sci 133(6):jcs236794. https://doi.org/10.1242/jcs.236794
33. Deng K, Thorn P (2022) Presynaptic-like mechanisms and the control of insulin secretion in pancreatic β-cells. Cell Calcium 104(104):102585. https://doi.org/10.1016/j.ceca.2022.102585
34. Bader E, Migliorini A, Gegg M et al (2016) Identification of proliferative and mature β-cells in the islets of Langerhans. Nature 535(7612):430–434. https://doi.org/10.1038/nature18624
35. Johnston NR, Mitchell RK, Haythorne E et al (2016) Beta cell hubs dictate pancreatic islet responses to glucose. Cell Metab 24(3):389–401. https://doi.org/10.1016/j.cmet.2016.06.020
36. Dorrell C, Schug J, Canaday PS et al (2016) Human islets contain four distinct subtypes of β cells. Nat Commun 7:11756. https://doi.org/10.1038/ncomms11756
37. Samols E, Stagner JI, Ewart RB, Marks V (1988) The order of islet microvascular cellular perfusion is B—A—D in the perfused rat pancreas. J Clin Investig 82(1):350–353. https://doi.org/10.1172/JCI113593
38. Nyman LR, Wells KS, Head WS et al (2008) Real-time, multidimensional in vivo imaging used to investigate blood flow in mouse pancreatic islets. J Clin Invest 118(11):3790–3797. https://doi.org/10.1172/JCI36209
39. Parnaud G, Hammar E, Ribaux P, Donath MY, Berney T, Halban PA (2009) Signaling pathways implicated in the stimulation of beta-cell proliferation by extracellular matrix. Mol Endocrinol 23(8):1264–1271. https://doi.org/10.1210/me.2009-0008
40. Gandasi NR, Barg S (2014) Contact-induced clustering of syntaxin and munc18 docks secretory granules at the exocytosis site. Nat Commun 5:3914. https://doi.org/10.1038/ncomms4914
41. Hogan MF, Hull RL (2017) The islet endothelial cell: a novel contributor to beta cell secretory dysfunction in diabetes. Diabetologia 60(6):952–959. https://doi.org/10.1007/s00125-017-4272-9
42. Peiris H, Bonder CS, Coates PT, Keating DJ, Jessup CF (2014) The beta-cell/EC axis: how do islet cells talk to each other? Diabetes 63(1):3–11. https://doi.org/10.2337/db13-0617

43. Sasson A, Rachi E, Sakhneny L et al (2016) Islet pericytes are required for β-cell maturity. Diabetes 65(10):3008–3014. https://doi.org/10.2337/db16-0365
44. Almaca J, Weitz J, Rodriguez-Diaz R, Pereira E, Caicedo A (2018) The pericyte of the pancreatic islet regulates capillary diameter and local blood flow. Cell Metab 27(3):630-644.e634. https://doi.org/10.1016/j.cmet.2018.02.016
45. Tamayo A, Gonçalves LM, Rodriguez-Diaz R et al (2022) Pericyte control of blood flow in intraocular islet grafts impacts glucose homeostasis in mice. Diabetes 71(8):1679–1693. https://doi.org/10.2337/db21-1104
46. Hayden MR, Sowers JR, Tyagi SC (2005) The central role of vascular extracellular matrix and basement membrane remodeling in metabolic syndrome and type 2 diabetes: the matrix preloaded. Cardiovasc Diabetol 4:9. https://doi.org/10.1186/1475-2840-4-9
47. Forbes JM, Cooper ME (2013) Mechanisms of diabetic complications. Physiol Rev 93(1):137–188. https://doi.org/10.1152/physrev.00045.2011
48. Cohrs CM, Chen C, Jahn SR et al (2017) Vessel network architecture of adult human islets promotes distinct cell-cell interactions in situ and is altered after transplantation. Endocrinology 158(5):1373–1385. https://doi.org/10.1210/en.2016-1184
49. Chen C, Chmelova H, Cohrs CM et al (2016) Alterations in β-cell calcium dynamics and efficacy outweigh islet mass adaptation in compensation of insulin resistance and prediabetes onset. Diabetes 65(9):2676–2685. https://doi.org/10.2337/db15-1718
50. Brissova M, Shostak A, Shiota M et al (2006) Pancreatic islet production of vascular endothelial growth factor-A is essential for islet vascularization, revascularization, and function. Diabetes 55(11):2974–2985. https://doi.org/10.2337/db06-0690
51. Lammert E, Gu GQ, McLaughlin M et al (2003) Role of VEGF-A in vascularization of pancreatic islets. Curr Biol 13(12):1070–1074. https://doi.org/10.1016/S0960-9822(03)00378-6